Representation of Spatial Functions in Geodesy Using B-Spline Wavelets with Compact Support

Rainer Mautz[1,2], Burkhard Schaffrin[1], Michael Schmidt[1,3], and C.K. Shum[1]

[1] Department of Civil and Environmental Engineering and Geodetic Science, The Ohio State University, Columbus, Ohio, USA

[2] Department of Astronomical, Physical and Mathematical Geodesy, Technical University of Berlin, Germany

[3] German Geodetic Research Institute (DGFI), Munich, Germany

Abstract. For the representation of a spatial function such as the topography or the geoid, scalar-valued spline wavelets may be used that are defined on a two-dimensional, but not necessarily planar domain. A certain type of spline wavelets is generated by B-splines, which can be implemented at different degrees: Degree 0 represents the Haar wavelet, degree 1 the linear B-spline wavelet or degree 3 the cubic B-spline wavelet. A non-uniform version of these wavelets allows us to handle data on a bounded domain without any edge effects. Using the piecewise linear version of B-spline wavelets, one may model the gravity field of the Earth by a patch-wise approach along a certain number of belts. This paper provides the basic ideas of the two-dimensional B-spline wavelet approach and gives an outlook for representing geodetic data.

Such a wavelet expansion represents data given on a grid exactly, if the number of wavelet coefficients is equal to the number of grid points. But data compression is advised and can be carried out quite easily by eliminating the wavelet coefficients with small magnitudes. There are very small deviations between the decompressed and the original data set.

A hierarchical decomposition not only allows an inexpensive calculation, but also a representation of different detail levels. Each level corresponds to a certain spatial frequency band, leading to a useful interpretation with regard to the frequency domain.

Keywords. B-splines, wavelets, multi-resolution representation, Kronecker product

1 Introduction

In geodesy one of the principal research foci is the efficient representation of the gravity field, the topography, or - more recently - of atmospheric data. With new requirements in terms of precision and new available sensors there is a fast growing amount of geodetic data to be analyzed. In the last decade the powerful and flexible tool known as “wavelet transform” has been established in geodesy, allowing the multi-resolution representation of multi-dimensional data. In this context, Salamonowicz (2001) and Schmidt (2001) among others have made various successful attempts to exploit wavelets.

A special kind of wavelets is generated by B-splines, offering useful properties such as compact support, semi-orthogonality, symmetry, and simplicity. In case of linear B-splines, the wavelet functions become biharmonic. The B-splines on a bounded interval were introduced by Chui and Quak (1992) whereas decomposition and reconstruction algorithms are presented in Quak and Weyrich (1994). Applications and user friendly algorithms can be found in Stollnitz et al. (1996). The mathematical background for functions on the sphere is described in Lyche and Schumaker (2000).

2 Generation of B-Splines

The B-spline functions are created recursively with an increase of the polynomial degree $d \in \mathbb{N}_0$ by one within each step. The iteration procedure is initialized by the piecewise constant characteristic function $\chi = \phi^0$ for the degree 0 spline,

$$\phi_k^0(x) := \begin{cases} 1 \text{ if } x_k \le x < x_{k+1} \\ 0 \text{ otherwise} \end{cases} \tag{1}$$

where x is the function variable and x_k are members of the knot sequence

$$\left(x_0, \ldots x_{2^j+2d}\right) = \tfrac{1}{2^j}\left(\underbrace{0,\ldots,0}_{\text{d+1 times}}, 1, 2, \ldots, 2^j-1, \underbrace{2^j,\ldots,2^j}_{\text{d+1 times}}\right) \tag{2}$$

where $j \in \mathbb{N}_0$ is the level of detail and $d \in \mathbb{N}_0$ denotes the polynomial degree of the splines. $\phi_{0,k}(x)$ means the B-spline scaling function of level zero, it is equivalent to the scaling

(= generating) function of the Haar wavelet. The index $k = 1,..., 2^j + d$ can be seen as a "shift" parameter. In order to get splines of higher degree $d > 0$, the recursion formula

$$\phi_k^r(x) := \frac{x - x_k}{x_{k+r} - x_k}\phi_k^{r-1}(x) + \frac{x_{k+r+1} - x}{x_{k+r+1} - x_{k+1}}\phi_{k+1}^{r-1}(x) \quad (3)$$

is used, where $r = 1,..., d$ denotes the recursion number. (3) can be seen as an interpolation between the neighboring $r + 1$ knots to knot x_k; the polynomial degree is incremented when $\phi^{r-1}(x)$ is multiplied by x. The fractions in (3) are taken to be zero, when their denominators are zero.

The knot values of the scaling functions of a level space j are stored in a matrix $\mathbf{\Phi}_j = (\phi_{j,i,k}) = (\phi_{j,k}(x_i))$, where each column represents a scaling function value for a certain location. $\mathbf{\Phi}_j$ is a m by $2^j + d$ matrix, where m represents the number of sampled data points and $2^j + d$ the number of scaling function values for level space j. Accordingly, $\mathbf{\Phi}_0$ denotes the whole space of level 0, including all shifted versions of the scaling function in the spatial domain. It has to be pointed out that the scaling functions of a level space are not overall identical shifted versions of each other. Due to multiple knots, given by the first $d + 1$ zero entries and the last $d + 1$ constant entries of the knot sequence (2), the interpolating scheme (3) creates endpoint interpolating B-splines. The first d scaling functions differ from the usual behavior of the inner scaling functions, avoiding edge effects at the boundaries of a finite data set. The non-uniformity of the scaling functions of level space $j = 2$ and degree $d = 3$ are shown in Figure 1.

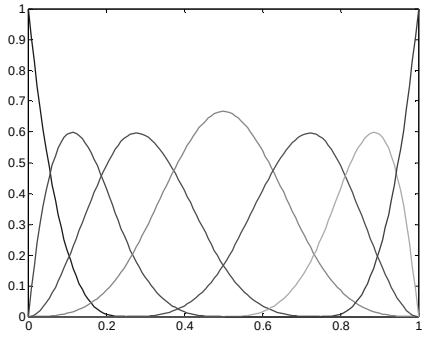

Fig. 1 Cubic B-spline Scaling functions of level $j = 2$

3 Multi-Resolution and Filter Bank

The scaling functions are refineable, since level spaces form nested subspaces, and consequently for all $j = 1,2,...$ there must exist a matrix $\mathbf{P}_j$ such that the two-scale relation

$$\mathbf{\Phi}_{j-1} = \mathbf{\Phi}_j \mathbf{P}_j \quad (4)$$

holds. The wavelet spaces are also subspaces of higher level spaces, thus there must also exist a matrix $\mathbf{Q}_j$ generating the wavelet matrix $\mathbf{\Psi}_{j-1}$ for the lower level j-1 fulfilling

$$\mathbf{\Psi}_{j-1} = \mathbf{\Phi}_j \mathbf{Q}_j. \quad (5)$$

The mathematical background for the generation of the **P** and **Q** matrices can be found in Quak and Weyrich (1994). Example matrices for **P** and **Q** are given in Stollnitz et al. (1996). This approach forms a semi-orthogonal B-spline wavelet basis, fulfilling the condition

$$\langle \phi_{j,k}, \psi_{j,l} \rangle = 0 \text{ for all } j, k, l, \quad (6)$$

which means that the wavelet functions are orthogonal to the scaling functions, but not to each other within one level.

With the conditions (4) - (6) and a given set of scaling functions, there are still a large number of possible **Q**-matrices. Out of these, we can construct the **Q**-matrix with a minimum number of nonzero entries, leading us to compactly supported wavelets.

Via the tensor product for level spaces, we can form the 2-D basis functions as follows:

$$\begin{aligned} &\phi(x,y) := \phi(x)\cdot\phi(y) && \text{scaling function} \\ &\psi_1(x,y) := \phi(x)\cdot\psi(y) && \text{vertical} \\ &\psi_2(x,y) := \psi(x)\cdot\phi(y) && \text{horizontal} \\ &\psi_3(x,y) := \psi(x)\cdot\psi(y) && \text{diagonal} \end{aligned} \quad \left.\right\} \text{ wavelet functions} \quad (7)$$

where $\phi(x)$ and $\phi(y)$ are the 1-D scaling functions for the x- and y-direction on the plane. The three types of 2-D wavelet functions are of different shape, enabling the absorption of vertical, horizontal or diagonal patterns in the data.

Let us assume $\mathbf{t} \in \mathbb{R}^2$ is a position vector. With the wavelet decomposition, the signal $y(\mathbf{t})$ is decomposed into a smoothed signal and a sum of different detail signals as follows:

$$y(\mathbf{t}) - e(\mathbf{t}) = \sum_{k\in\mathbb{Z}^2} c_{j_{\min},k}\tilde{\phi}_{j_{\min},k}(\mathbf{t}) + \sum_{j=\min}^{J}\sum_{\eta=1}^{3}\sum_{k\in\mathbb{Z}^2} d_{j,k}^{\eta}\tilde{\psi}_{j,k}^{\eta}(\mathbf{t}) \quad (8)$$

The observational error of $y(\mathbf{t})$ is denoted by $e(\mathbf{t})$, which will be set to zero if the number of coefficients is equal to the number of data points given on a grid. The adjustment of (8) leads to the determination of the unknown scaling function coefficients $c_{jmin,k}$ as well as the wavelet coefficients $d^{\eta}_{j,k}$. The different levels of detail are denoted by the index j. Wavelet coefficients with a larger j represent higher detail levels

expressing the high-frequency part. The index η sums up the three directions introduced in (7) and the index k shifts the wavelets to different locations on the plane. For the reconstruction of the signal the dual scaling and wavelet functions have to be used, denoted by a tilde.

In fact, the calculation of the coefficients can be carried out in a simple and computationally efficient way, using a filter-bank procedure for decomposition. One step of this recursive process is given by

$$\left[\mathbf{P}_j \ \mathbf{Q}_j\right]^{-1} \mathbf{C}_j \left[\mathbf{P}_j \ \mathbf{Q}_j\right]^{-1^{\mathrm{T}}} = \begin{bmatrix} \mathbf{C}_{j-1} & \mathbf{D}^1_{j-1} \\ \mathbf{D}^2_{j-1} & \mathbf{D}^3_{j-1} \end{bmatrix}. \qquad (9)$$

Starting from the scaling coefficients of the highest level $\mathbf{C}_J$, all scaling and wavelet coefficients of lower levels can be derived. The scaling coefficients are stored in form of a $2^j + d$ by $2^j + d$ matrix $\mathbf{C}_j$ according to their spatial position, whereas the three sub matrices $\mathbf{D}^{\eta}_{j-1}$ contain the wavelet coefficients of the three directional components. The matrices $\mathbf{P}$ and $\mathbf{Q}$ can be seen here as refinement matrices and do not depend on the data. The synthesis of all detail signals is done with the inverse filter-bank procedure

$$\mathbf{C}_j = \left[\mathbf{P}_j \ \mathbf{Q}_j\right] \begin{bmatrix} \mathbf{C}_{j-1} & \mathbf{D}^1_{j-1} \\ \mathbf{D}^2_{j-1} & \mathbf{D}^3_{j-1} \end{bmatrix} \left[\mathbf{P}_j \ \mathbf{Q}_j\right]^{\mathrm{T}}, \qquad (10)$$

where the scaling coefficients of the highest level can be reobtained in the last step. The highest levels J_x and J_y for the data in x- and y-direction may not necessarily be the same, when the data are rather on a rectangle then on a square. In order to keep clarity, this is not regarded here.

4 Kronecker Product for 2-D data

When implementing a filter-bank procedure as described in the previous chapter, the fist step is to adjust the system of linear equations $\mathbf{y} - \mathbf{e} = \mathbf{\Phi}\, \mathbf{c}_J$ in order to get the vector for the unknown coefficients of the highest level J from a given observation vector $\mathbf{y}$. Here, the coefficients $\mathbf{c}_J$ form a vector $\mathbf{c}_J = vec(\mathbf{C}_J)$, where the *vec*-operator writes the columns of $\mathbf{C}_J$ one underneath the other. With the covariance matrix of observations $D(\mathbf{y}) = \sigma^2\, \mathbf{I}$, the least-squares solution is

$$\mathbf{c}_J = (\mathbf{\Phi}^{\mathrm{T}}\, \mathbf{\Phi})^{-1}\, \mathbf{\Phi}^{\mathrm{T}}\, \mathbf{y}. \qquad (11)$$

The matrix $\mathbf{\Phi}$ is a large n by m matrix where n is the number of observations and $m = (2^J+d)^2$ the number of coefficients. d again denotes the polynomial degree. Using (11) allows handling scattered data, but only with a large storage and calculation effort. In order to handle large 2-D data efficiently on a raster, the matrix $\mathbf{\Phi}$ can be split up into the two 1-D scaling matrices $\mathbf{\Phi}_x$ and $\mathbf{\Phi}_y$ for x- and y-direction

$$\mathbf{\Phi} = \mathbf{\Phi}_y \otimes \mathbf{\Phi}_x, \qquad (12)$$

where the symbol $\otimes$ stands for the Kronecker product of matrices. Substituting $\mathbf{\Phi} = \mathbf{\Phi}_y \otimes \mathbf{\Phi}_x$ in (11) we obtain

$$\mathbf{c}_J = [(\mathbf{\Phi}_y \otimes \mathbf{\Phi}_x)^{\mathrm{T}} (\mathbf{\Phi}_y \otimes \mathbf{\Phi}_x)]^{-1} (\mathbf{\Phi}_y \otimes \mathbf{\Phi}_x)^{\mathrm{T}}\, \mathbf{y}\,. \qquad (13)$$

After applying the Kronecker product laws, e.g. given by Koch (1997, p.19, 41), we obtain

$$\mathbf{C}_J = (\mathbf{\Phi}_x^{\mathrm{T}}\, \mathbf{\Phi}_x)^{-1}\, \mathbf{\Phi}_x^{\mathrm{T}}\, \mathbf{Y}\, \mathbf{\Phi}_y\, (\mathbf{\Phi}_y^{\mathrm{T}}\, \mathbf{\Phi}_y)^{-1} \qquad (14)$$

with $\mathbf{y} = vec(\mathbf{Y})$. The matrix $\mathbf{Y}$ represents equidistantly spaced data points. In order to demonstrate the computational benefit of (14) assume a 1024 × 1024 dataset $\mathbf{Y}$. Using equation (14) the calculation of $\mathbf{\Phi}_x^{\mathrm{T}}\, \mathbf{\Phi}_x$ takes about 10^9 multiplications, which is much less than 10^{18} multiplications for $\mathbf{\Phi}^{\mathrm{T}}\, \mathbf{\Phi}$ in (11).

Using the Kronecker product approach, one can efficiently view the three directional detail signals by

$$\begin{aligned} \mathbf{G}_{j,1} &= \mathbf{\Phi}_{x,j} \mathbf{D}^1_j \mathbf{\Psi}^{\mathrm{T}}_{y,j} \\ \mathbf{G}_{j,2} &= \mathbf{\Psi}_{x,j} \mathbf{D}^2_j \mathbf{\Phi}^{\mathrm{T}}_{y,j} \\ \mathbf{G}_{j,3} &= \mathbf{\Psi}_{x,j} \mathbf{D}^3_j \mathbf{\Psi}^{\mathrm{T}}_{y,j}. \end{aligned} \qquad (15)$$

The wavelet coefficient matrices $\mathbf{D}$ are determined by (9). The complete detail signal of level j is $\mathbf{G}_j = \mathbf{G}_{j,1} + \mathbf{G}_{j,2} + \mathbf{G}_{j,3}$ and the reconstructed data result from the sum over all $\mathbf{G}_j$.

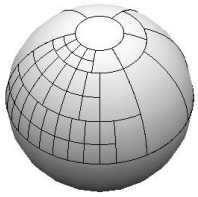

Fig. 2 Example of an Igloo structuring approach with different subdivision deepness for different regions

The construction of spherical pseudo-wavelets can be done by a Mercator projection from a spherical patch in isometric latitude q and longitude λ to the standard planar quadrangle $-1 \le x \le +1$ and $-1 \le y \le +1$, and vice versa. The wavelet analysis is then performed in the plane for each patch separately. The mathematical background can be found in Schaffrin et al. (2002), including techniques for a decomposition

of the sphere by an Igloo data structuring approach. See also Figure 2.

5 Data Analysis and Compression

Wavelets localize both in space and frequency domain. But, due to the "Heisenberg Uncertainty Relation", it is not possible to determine an exact frequency at a specific position. The variations in space and frequency for a function are measured by the Heisenberg Box, whose optimal size is 2.0 when applied to the Gauss function. For the linear B-spline wavelets the box size becomes 3.88 which is fairly good. The cubic B-spline wavelets have an almost optimal box size of 2.02, allowing an excellent analysis of data in terms of location and frequency content. Every level of detail represents a certain frequency band; thus, the values of the wavelet coefficients will directly reflect the frequency content at different locations. Furthermore, every level of detail can be split up into diagonal, horizontal and vertical signals, allowing further investigations of directional structures in the data. Figure 3 shows an analysis of a detail signal based on linear B-splines.

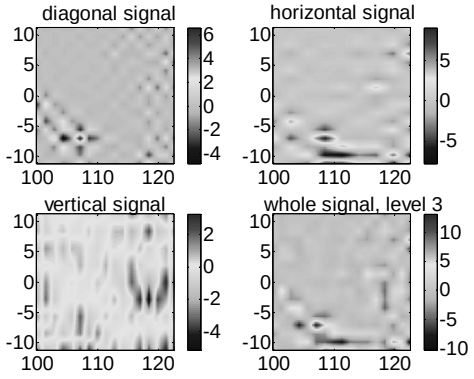

Fig. 3 Diagonal, horizontal and vertical detail signals of geoid undulations on a 22.5° by 22.5° patch in the Indian Ocean for level 3. The graph in the lower right represents the complete detail signal of that level.

The magnitude of the coefficients in the decomposed stage of the signal varies broadly. If the histogram of all wavelet coefficients has a high peak for small values, a large number of coefficients can be neglected by a thresholding process without any major loss of information. Such a data compression leads to relatively small root mean square deviations for high compression factors. An application of B-spline compression on geoid undulations for a 22.5° by 22.5° patch in the Indian Ocean has been carried out in Schaffrin et al. (2002). In this example a negligence of 90% of the wavelet coefficients leads to a root mean squared deviation from the uncompressed signal of ± 2.4 cm; see also Table 1.

Table 1. Different compression values, the resulting root mean squared deviations and the maximal deviations δ_{max}

Compression [%]	no. of remaining coefficients	rms deviation [m]	$\lvert\delta_{max}\rvert$ [m]
0.0	66049	0	0
75.0	16512	0.0074	0.03
90.0	6605	0.024	0.10
95.0	3303	0.054	0.23
99.0	661	0.39	2.0

Conclusions

The B-spline wavelets allow multi-resolution representations of geodetic data. The presented approach allows representing two-dimensional signals. A transfer from the plane to the sphere for spatial functions in order to model topography or gravity data is possible. With the help of the Kronecker product for scaling and wavelet functions in different directions, the computational effort may be reduced drastically if the data is given on an equidistant grid. Useful features as data analysis and data compression can be carried out successfully.

References

Chui, C.K., E. Quak (1992): *Wavelets on a Bounded Interval*; in: Numerical Methods in Approximation Theory, Vol. 9, (D. Braess and L. Schumaker, Eds.), Birkhäuser: Basel, Boston, Berlin, pp. 53-77

Koch, K. (1999): *Parameter Estimation and Hypothesis Testing in Linear Models*. Springer: Berlin, etc.

Lyche, T., L. Schumaker (2000): *A Multiresolution Tensor Spline Method for Fitting Functions on the Sphere*, SIAM J. Sci. Comput. 22 (2000), pp. 724-746

Quak, E., N. Weyrich (1994): *Decomposition and Reconstruction Algorithms for Spline Wavelets on a Bounded Interval*. Applied and Computational Harmonic Analysis 1, pp. 217-231

Salamonowicz, P.H. (2001): *A wavelet-based gravity model with an application to the evaluation of Stokes' integral*; in: Gravity, Geoid and Geodynamics 2000 (M.G.Sideris, ed.), IAG-Symp. Vol.123, Springer: Berlin etc., pp. 85-90

Schaffrin, B., R. Mautz, C.K. Shum, H. Tseng (2002): *Towards a Spherical Pseudo-Wavelet Basis for Geodetic Applications.* Computer-Aided Civil and Infrastructure Engineering, (accepted for publication)

Schmidt, M (2001): *Basic principles of the wavelet analysis with applications to geod*esy (in German), Habilitation thesis, Shaker: Aachen.

Stollnitz, E., T. DeRose and D. Salesin (1996): *Wavelets for Computer Graphics*, M. Kaufmann: San Francisco